1-12-2010

Influence of shear stress in perfusion bioreactor cultures for the development of three-dimensional bone tissue constructs: a review.

Ryan J. McCoy
Royal College of Surgeons in Ireland

Fergal J. O'Brien
Royal College of Surgeons in Ireland, fjobrien@rcsi.ie

— Use Licence —

Influence of Shear Stress in Perfusion Bioreactor Cultures for the Development of Three-Dimensional Bone Tissue Constructs: A Review

Ryan J. McCoy, Eng.D.,[1,2] and Fergal J. O'Brien, Ph.D.[1,2]

Bone tissue engineering aims to generate clinically applicable bone graft substitutes in an effort to ease the demands and reduce the potential risks associated with traditional autograft and allograft bone replacement procedures. Biomechanical stimuli play an important role under physiologically relevant conditions in the normal formation, development, and homeostasis of bone tissue—predominantly, strain (predicted levels *in vivo* for humans $<2000\,\mu\varepsilon$) caused by physical deformation, and fluid shear stress (0.8–3 Pa), generated by interstitial fluid movement through lacunae caused by compression and tension under loading. Therefore, *in vitro* bone tissue cultivation strategies seek to incorporate biochemical stimuli in an effort to create more physiologically relevant constructs for grafting. This review is focused on collating information pertaining to the relationship between fluid shear stress, cellular deformation, and osteogenic differentiation, providing further insight into the optimal culture conditions for the creation of bone tissue substitutes.

Introduction

CURRENTLY, UP TO 4 million bone replacement procedures are conducted annually, with over 50% requiring the use of bone graft materials, a market expected to be worth $U.S. 2.5 billion. This makes bone second only to blood on the list of transplanted materials. Increasing limitations with the supply of bone grafts from the traditional autograft and allograft routes, which themselves contain drawbacks and risks, including the restricted amount of bone removal, additional invasive surgery, risk of infectious disease transmission, and lack of available donors, have elevated the demand for alternative graft materials with properties suitable for clinical use. Bone tissue engineering may provide an alternative solution; however, the development of an *in vitro* bone tissue-engineered substitute capable of integrating into the host has yet to reach fruition.

Interdisciplinary collaboration between the engineering and life science communities, aiming to build upon understanding of the founding principles in each field, seeks to provide mechanically apt biocompatible composites with desired architectures (scaffolds), in combination with bio-regulatory factors (chemical and mechanical cues) and/or cells to create tissue *ex vivo* or induce growth of tissue *in vivo* (tissue engineering and regenerative medicine). Utilization of scaffolds on their own (cell free) has shown some promise in aiding the regeneration of bone *in vivo* and providing a solution for the aforementioned unmet clinical need.[1,2] How-

ever, the length of time needed to achieve healing is still substantial as cellular infiltration into the scaffold and conditioning of the microenvironment is a slow process. Multipotent progenitor cells responsible for tissue in-growth and remodeling inherently possess the ability to differentiate along numerous lineages. The cascade of environmental cues (chemical signals, mechanical stimuli, hypoxia, etc.) experienced by these progenitor cells defines the differentiation process and determines the final cell phenotype. Identification of this hierarchal structure of cues and their timing within the cascade is a key focal point of tissue engineering and regenerative medicine research and is beginning to provide an artificial means of growing tissue *in vitro* that when implanted *in vivo* yields an accelerated healing time.[3] Alternatively, such bone tissue constructs may provide a foundation for studying various aspects of bone physiology,[4] cell–matrix interactions,[5,6] mechanotransduction, tumor cell behavior,[7,8] and bone infection, satisfying the demand for improved physiologically relevant *in vitro* three-dimensional (3D) culture systems in these fields and thereby potentially providing a means for a reduction in the number of animal-based studies necessary.

Static culturing of progenitor cells in porous scaffolds and maturing them in the presence of differentiation media (chemical cues) along an osteogenic lineage[9–16] is the most simplistic methodology of developing bone tissue constructs for *in vivo* implantation. However, this approach neglects the important role mechanical cues play under physiologically

[1]Department of Anatomy, Royal College of Surgeons in Ireland, Dublin, Ireland.
[2]Trinity Centre for Bioengineering, Trinity College Dublin, Dublin, Ireland.

relevant conditions in the normal formation, development, and homeostasis of tissues. Biomechanical stimuli have been recognized as an important part of *in vivo* bone remodeling for almost a century[17] and necessary for stimulating cells to elicit correct cellular differentiation/functioning.[18] The substantial loss of bone during spaceflight[19,20] or after significant periods of bed rest,[21] where reduced mechanical loading environments are experienced for long periods of time, supports the argument for the importance of biomechanical stimuli in bone homeostasis. Bone is predominately subjected to two forms of biomechanical stimuli that control turnover: strain (predicted levels *in vivo* for humans $<2000\,\mu\varepsilon$[22]), caused by physical deformation, and fluid shear stress (0.8–3 Pa), generated by interstitial fluid movement through lacunae caused by compression and tension under loading. Investigations into the functional response of bone to strain-based loading regimes that cause cellular deformation via hypotonic swelling, hydrostatic pressure, or uniaxial or biaxial strain have been reviewed comprehensively by Duncan and Turner.[23]

This review is focused on collating information pertaining to the relationship between fluid shear stress, cellular deformation, and osteogenic differentiation, providing further insight into the optimal conditions for the creation of bone tissue substitutes.

Fluid Shear Stress and Mechanotransduction in Two-Dimensional and Three-Dimensional Systems

Fluid shear stress is created by fluid movement tangential to the face of a surface, for incompressible Newtonian fluids the shear stress will be linearly proportional to the velocity gradient perpendicular to the plane of shear; the proportionality constant equates to the fluid viscosity. The governing equation can be written as

$$\tau_{ij} = \mu \left(\frac{\partial v_i}{\partial x_j} + \frac{\partial v_j}{\partial x_i} \right),$$

where τ_{ij} = shear stress on the ith face of a fluid element in the jth direction; μ = fluid viscosity; v_i and v_j = velocity in the ith and j^{th} directions, respectively; and x_i and x_j = the ith and j^{th} direction coordinates, respectively.

Various experimental setups, parallel plate flow chambers,[24–32] rotating disc[33–37] or radial flow devices,[38,39] cone and plate viscometers,[40] jet impingement[24] systems, and microfluidic apparatus,[41,42] have been utilized for applying flows in two-dimensional (2D) systems and examining the effect of shear stress on cell monolayers. In 3D systems, fluid agitation is essential in reducing mass transfer constraints associated with concentration gradients at the fluid-construct boundary interface[43,44]; it has long been known that diffusion of oxygen and soluble nutrients to the construct core can become critically limited in longer term static cultures as tissue growth and extracellular matrix (ECM)/mineralization occurs,[45,46] resulting in a necrotic core with an external shell of viable tissue. Numerous bioreactor types have been designed for 3D tissue engineering applications and their roles have been reviewed by Martin *et al.*,[47] spinner flasks, rotating wall bioreactors, hollow fiber membrane systems, and perfusion rigs being the most common. Several perfusion bioreactor styles have been devised to date[43,48–51] (Fig. 1). Perfusion appears to offer the greatest benefits as fluid is forced through the entire construct creating a more homogeneous microenvironment, rather than just improving convection at the construct surface. Additionally, the development of complementary nondestructive imaging techniques via microcomputed tomography to monitor mineralization allowing *in situ* quantitative analysis of mineralized particle size, number, and distribution offers a powerful tool for evaluating the effects of cell type, scaffold material, architecture, or bioreactor flow conditions on the level of osteogenesis.[52]

The highly porous scaffolds utilized for bone tissue engineering within these systems would ideally have the potential to be load bearing once incorporated *in vivo*. However, materials that are superior in terms of mechanical properties are often inferior in terms of biological compliance and thus a trade off has to be made. Currently, biologically superior materials are favored with efforts to increase the mechanical properties a common focus, at least to a point that allows surgical handling without damage. For example, collagen-glycosaminoglycan scaffolds developed by Yannas *et al.*[53]

FIG. 1. Example of a perfusion bioreactor setup as used in our laboratory to apply biomechanical stimuli (not drawn to scale) with an accompanying enlarged cross section of the scaffold chamber (not drawn to scale). To obtain perfuse flow the scaffold is set within an O-ring that limits the diameter of the flow path to that area in which the scaffold is present. The medium is pumped from the syringe pump, through the scaffold chamber and into the medium reservoir. The rate of fluid flow is controlled automatically by the syringe pump to user-defined levels and the nature of the flow type (pulsatile, steady, and oscillatory) can be determined by setting step changes in the flow, which approximate to sinusoidal waveforms. Image was reproduced from Jungreuthmayer *et al.*[102] with permission from Elsevier.
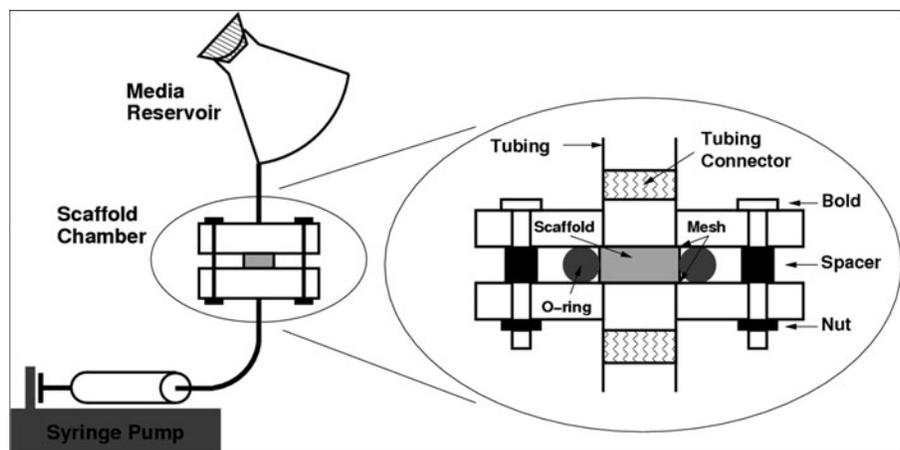
are being adapted for bone tissue engineering in our laboratory[54–56] through incorporation of calcium phosphate or nano-hydroxyapatite into the collagen structure and thereby improving the mechanical strength. However, these porous scaffolds still contain highly irregular geometries as a consequence of freeze-drying[57,58] or salt-leaching[14] manufacturing processes, resulting in nonuniform flow profiles and hence shear stress distributions (with variations greater than one order of magnitude present) even when uniform inlet velocities[59–61] are applied. This would not be problematic if broad limits are acceptable for the required shear stress to stimulate differentiation along a particular lineage, but may result in heterogeneity of cellular responses if a narrower operating range is deemed specific for osteogenesis. Changing the porosity/geometric architecture of these scaffolds or manipulating the perfusion flow-rate will allow the extent of the biomechanical stimuli experienced by the cells to be controlled to some degree. Techniques such as rapid prototyping or solid free-form fabrication that allows the controlled fabrication of complex geometries with regular pore structures are becoming more commonly applied to the design of tissue engineering scaffolds in recent years, potentially offering a solution to the aforementioned problem of irregular geometries leading to broad shear stress distributions; these approaches/systems have been reviewed in depth by numerous authors.[62–65] Their lack of uptake to date is primarily a function of the reduced levels of biocompatibility associated with the polymer materials that the scaffolds are constructed from. However, technological advances that allow the rapid prototyping or solid free-form fabrication of biological materials or the generation of composite materials, for example, by lypophilizing collagen into macroporous polymer structures,[52] may see an increase in the use of this technology for clinically driven applications.

Translating the physical force applied at the cell surface into a biological signal is termed mechanotransduction. The mechanisms responsible for mechanotransduction are still an active area of research and have been reviewed in depth elsewhere.[66–68] Principally two major theories exist. First, responses are based on the regulation of stretch-activated ion channels, where force-induced changes in the plasma membrane result in an influx/efflux of ions into/out of the cell. Second, responses are based on integrin-initiated cytoskeleton deformations. Integrins are a subpopulation of heterophylic cell adhesion molecules, which are major transmembrane proteins connected to the cellular cytoskeleton that cluster at focal adhesion points on the cell surface. They are noncovalently linked heterodimers consisting of a single α and β subunit. There are a total of 18 different α subunits and 9 different β subunits that can combine to form 24 different integrins. Different integrins are linked to an array of signaling pathways whose activation leads to a range of cellular responses.[69] Their role is to bind ECM ligands forming an integrin-ligand bond; the two major integrins responsible for binding to collagen, the largest source of ECM in bone, are α1β1 and α2β1.[69] Resistance to the application of an external force occurs at the point of integrin-ligand bonding, allowing transmission of the force across the plasma membrane into the cell interior, either causing direct deformation of the cytoskeleton or indirect movement of internal organelles, thereby triggering a response. Studies have shown that retention of cytoskeletal tension is necessary for activation of genes involved in osteogenic pathways.[70,71]

Cell Attachment: Morphology and Strength in 2D and 3D Systems

Cell attachment morphology has the potential to influence the dynamics of surface-cell-flow relationships and thus impact upon the magnitude of cytoskeletal deformations. For conventional 2D experiments cells are uniformly attached in a manner parallel to the culture surface creating monolayers. Attachment strengths are dependent on surface properties and cellular characteristics, with critical shear stress levels (the shear stress level required to remove 50% of attached cells) typically >1 Pa and increasing toward 100s of pascals, depending on the time frame of shear stress exposure in the study. Numerous groups have shown that increasing the hydrophilicity or wettability of surface materials enhances cellular attachment strength.[25,28,30,31,37,41] In addition to the surface chemistry, Deligianni et al.[33] showed that increasing surface roughness aided attachment strength, whereas further augmentation of the adhesion surfaces, by coating with biological ligands, has yielded improvements dependent upon ligand type[24,27,35] and proportional to ligand density.[26,32,36,39,42] Xiao and Truskey demonstrated that maintaining the native conformation of the ligand appears to be advantageous in conferring stronger ligand-receptor bonds[32] in comparison to using linear fragments. From a cellular perspective, cell type,[29] seeding density,[40] length of attachment time before shear force application,[27] and the number of cellular focal adhesion points[39] all influence the ultimate detachment strength. However, if the receptor-ligand bond is stronger than the matrix, this does not necessarily negate the possibility of cellular detachment in response to shear stress; Engler et al.[34] showed that matrix failure as a consequence of cellular attachment (through increased resistance to flow) can also account for cellular loss. In general, the levels of shear stress required to induce cellular detachment in 2D are orders of magnitude greater than those expected to cause osteogenesis in vivo (0.8–3 Pa) and hence expected to occur in vitro; therefore, cellular loss from in vitro 2D systems through the application of fluid shear stress during osteogenic investigations is not a major concern.

In highly porous scaffolds (3D systems), cells attach to surfaces in one of two morphologies: flatly or bridged[72,73] (Fig. 2). Bridged cells are expected to experience greater level of cytoskeletal deformation at an equal shear stress because they are orientated normal to the flow direction. Quantitative analysis of cell attachment morphology and ratio of morphology types in 3D porous scaffolds has been limited to date. However, McMahon,[73] through confocal microscopy, has suggested that 75% of cells are attached in a bridged morphology and 25% as a flat morphology (for a collagen-glycosaminoglycan scaffold of pore size 95 μm and porosity >98%). Values for the attachment strength of bridged cells in porous scaffolds have yet to be published, but one can hypothesize, based on the information gained from 2D systems, that they would be substantially weaker; reduced contact area leading to fewer receptor-ligand bonds, plus an increased resistance to flow, as cells may orientate normal to the flow direction. Additionally, the procedures involved in the preparation of biocompatible scaffolds, such as blending, freeze-drying, and dehydrothermal cross-linking, may alter the conformation of proteins present, reducing potential
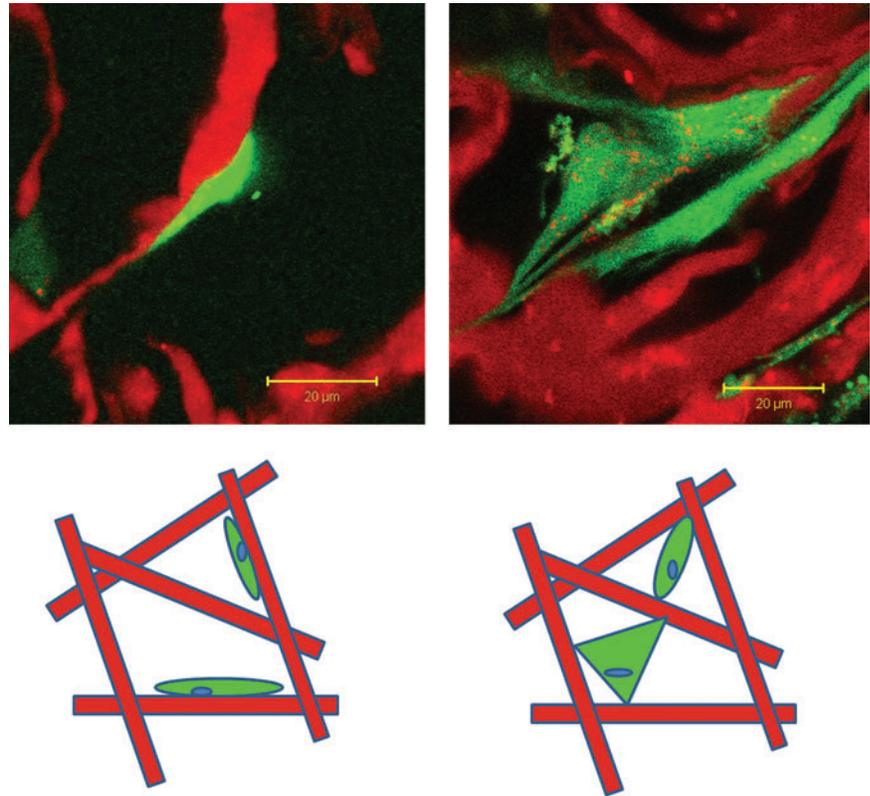
FIG. 2. Top: fluorescent microscopy images showing cells attached either predominantly flatly to collagen struts (left) or in a bridged manner (right). Bottom: schematic diagram of attachment morphologies with flatly attached on the left and bridged (either dual or multiattachment points) on the right. For both the microscopy images and schematics, the collagen structure is depicted in red and cell cytoplasm in green. Color images available online at www.liebertonline.com/ten.

integrin-ligand interactions. Experimental evidence corroborating this can been seen from published studies; Jaasma and O'Brien,[74] Partap et al.,[75] and Plunkett et al.[76] all experienced 40%–50% cell loss at shear forces two to four orders of magnitude (8×10^{-4} to 2×10^{-2} Pa) below the lowest seen in 2D experiments for a 49 h time frame.

If maintaining high seeding levels is deemed important to the success of *in vitro* bone tissue formation, then either scaffold design will need to ensure that primarily flatly attached cells are present so that knowledge from 2D systems can be directly translated or re-analysis pertaining the operational shear stress range for bridged cells needs to be undertaken.

Flow Application: Type and Timing

Although *ex vivo* experimental setups aim to mimic the *in vivo* environment, the use of physiologically relevant flow patterns is nominal, with steady state flow being preferred. When physiologically relevant flow patterns have been explored, comparisons are often difficult as single flow types with respect to no flow controls are studied in individual systems. In instances where flow types have been compared side by side, the consensus is mixed; data from Sharp et al.[77] suggest that pulsatile flow is best for the upregulation of bone sialoprotein (BSP), osteocalcin (OC), and bone morphogenetic proteins 2 and 7 (BMP2/7), and the downregulation of transforming growth factor-β_1; Jaasma and O'Brien[74] highlighted that pulsatile flow is best for the upregulation of cyclooxygenase-2 (COX-2), whereas oscillatory flow produces the greatest increase in prostaglandin E_2 (PGE$_2$). There is some evidence to suggest that constant stimulation of cells from

biomechanical stimuli, irrespective of flow type, leads to quiescence of the cellular response: cellular desensitization. The continued application of stress results in tolerance of the conditions by the cell, switching off the given response. Rest insertion (or low flow) periods between bouts of higher shear stress (for various flow types) have been explored by a number of authors in an effort to negate cellular desensitization and appears to lead to enhancement in expression of some genes but not others; increased expression levels of osteopontin (OPN),[75,76,78,79] BSP,[78] and PGE$_2$[74,80,81] were observed (with the exception of the study by Kreke et al.,[80] where there was no change compared to continuous flow for these genes), whereas collagen 1 (Col1),[74–76,80] alkaline phosphatase (ALP),[75,76,78,79] and COX-2[76] showed no apparent influence from rest insertion. Thus, from the literature reviewed, no conclusive consensus on the influence of flow type can be drawn, but rest insertion appears beneficial for osteoinductive approaches.

The timing of shear stress application is also a critical point for consideration. Cellular responses to shear stress can range from within seconds, as measured by cellular influxes of calcium,[82–84] to weeks, based on mineralized matrix deposition.[43,85–87] The duration and frequency of shear stress required to ensure commitment along a particular lineage is still being ascertained. In the majority of the literature surveyed, an attachment time of 24–72 h was allowed before the application of shear stress. In some instances, dynamic seeding[88,89] of cells was conducted in an effort to improve cell distribution within the scaffold, followed by either a static period or low flow period to enhance cell attachment strength or increase proliferation (cells may have been cultured in normal or differentiation medium for up to 14 days

before initiation of the stress). In most cases, however, differentiation medium was only used upon the onset of stress or poststress. Shear stress was usually applied for <48 h in the context of short-term studies or for 7–21 days for longer term studies, with cells being analyzed usually immediately after stress (within 24 h) or after 7–14 days culture poststress in static conditions (Table 1). Table 1 shows a summary of the above information for studies looking at differentiation of cells toward an osteogenic lineage and additionally includes information relating to the shear stress levels studied, the cell lines used, the bioreactor types employed, and the flow type.

Shear Stress and Osteogenic Differentiation

A wealth of literature exists for nonhuman[70,71,77,78,80,82,90–93] cell lines/primary cells and a limited amount pertaining to human[83,94–96] cell lines/primary cells, for mesenchymal stem cells (MSCs)[70,78,77,83,90,92,94,96] (such as murine mesenchymal progenitor cells) (C3H10T1/2), rat bone marrow stromal cells, adipose tissue-derived MSCs, or human MSCs and non-MSC[71,80,82,91,95] cell types, detailing the impact of fluid shear stress on directing commitment toward an osteogenic lineage for 2D systems (Fig. 3). Irrespective of the experimental conditions, shear stress positively increased expression levels of BSP,[77,78,80] OPN,[77,78,80,82,94] OC,[77,93] PGE$_2$,[71,80,91,96] Col1,[77,80,96] and nitric oxide[71,90,96] in multiple studies, whereas studies by Li *et al.* and McGarry *et al.* showed statistically insignificant changes in the levels of Col1[94] and PGE$_2$,[71] respectively. ALP[78,90,91] expression was not affected by the application of shear stress, whereas individual investigations evaluating COX-2,[90] Runx2,[70] BMP2/7, Sox9,[70] and peroxisome proliferator activated receptor gamma (PPARγ)[70] showed upregulation of gene or protein expression as a consequence of shear stress application, whereas its influence was negative or even suppressive for expression of BMP4,[77] COX1,[90] and transforming growth factor-β$_1$.[77] The variation in cell types used, culture conditions, and experimental platforms has increased the complexity of prizing out the importance of the role of fluid shear stress; nevertheless, it appears that a range of 0.1–0.5 Pa is most successful, and in some instances, values as high as 2 Pa have yielded positive responses, showing a good correlation with the levels of shear stress expected to occur *in vivo* (0.8–3 Pa).

For 3D culture, fluid shear stress experiments have been almost exclusively nonhuman[43,74–76,81,85,86,97,98] cell line orientated, with only a single study using a human[87] cell source (Fig. 3); only a minority of studies focused on MSC[43,85–87] cell types. These bodies of work suggest that osteogenic differentiation, as determined by increases in expression of ALP,[43,85,87,97,98] PGE$_2$,[74,76,81] OPN,[43,74–76] OC,[85,98] COX-2,[74,76] RunX2,[98] Col1,[97] and mineralized matrix production,[43,85,87,97] can be achieved with shear stresses in the range 1×10^{-4} to 1.2 Pa. The majority of work was focused in the 1 to 5×10^{-2} Pa range, which is at least an order of magnitude below the average for 2D culture and up to two orders of magnitude lower in some cases (other groups[99–101] have observed osteogenic differentiation within 3D systems but shear stresses were not quantified making comparison of the data unfeasible). These values are also orders of magnitude below those expected to cause differentiation *in vivo*, suggesting that the influence of ECM and mineralization *in vivo* may reduce the sensitivity to shear stress, by reducing the levels of cell deformation, as the cell is encased; further studies will be required to determine if this is the reason. As the knowledge space regarding differentiation as a function of morphological attachment type and shear stress is further populated, a clearer indication of the applicable magnitude of shear stress for the induction of osteogenic differentiation of human cells lines, in porous scaffolds, will be derived.

For the induction of osteogenesis, the difference in order of magnitude between 2D and 3D is ∼10–50 based on the midrange/most common values (0.5 Pa for 2D; 0.01–0.05 Pa for 3D), which ties into computational data produced by Jungreuthmayer *et al.*,[102] where the difference in the magnitude of the von Mises stresses (1.3 mPa for flat cells and 34 mPa for bridged cells) between flat and bridged cells is of the same order (for a scaffold of 120 μm pore size), supporting the idea that the level of cellular (cytoskeletal) deformation may play a key role in controlling differentiation. Previous work by Jaasma *et al.*[103] has shown that cells can alter their mechanical stiffness in an effort to regulate the impact of cellular deformation and hence mechanosensitivity, in an effort to control tissue structure and function; exposure to shear stresses in the range of 1–2 Pa (in a 2D system) caused an increase in the cell stiffness that was maintained for 70 min postshear. Jackson *et al.*[104] further showed that this increase in mechanical stiffness was directly related to the cytoskeleton, with the actin cytoskeleton cross-linking proteins alpha-actinin and filamin increased in osteoblasts responding to mechanical loading. Thus, it is appears that the cell cytoskeleton is a key component in the transduction of fluid forces to cellular responses.

Shear Stress and Angiogenesis

Bone tissue constructs once removed from the culture environment of the perfusion bioreactor are intended to be implanted into the patient. If substantial growth of tissue has been achieved *in vitro*, then nutrient deprivation of cells in the construct core may occur once implanted, as vascularization of the construct by the host, which provides a source of oxygen and nutrients, will be time consuming; this does not bode well for a positive clinical result. Potentially, this may be reduced if a vascularized construct can be created *in vitro*, allowing integration into the host quicker. In addition to bone, mechanical stimuli have been shown to influence the differentiation of other tissues in the body; for example, cyclic distension for the formation of arteries,[105–107] dynamic compressive loading for the formation of cartilage,[108–111] and uniaxial strain or axial compression/tension and torsion for ligament growth.[112] Directing cells toward an angiogenic (endothelial cell) lineage using shear stress is no exception. Similarly to bone, nonhuman[113–123] and human[124–128] cell lines have been studied, with the source of the progenitor cell lines being different to the bone studies. They almost all exclusively used 2D platforms (artificial capillary tube structures have been considered 2D in this review; a rolled up monolayer). A range of shear stresses between 0.01 and 2.5 Pa were explored, with the majority showing success at the higher end of the scale, >1.2 Pa.

Optimal Culturing Strategy

Perfusion culture for tissue engineering enhances nutrient transport and provides biomechanical cues. The question remains regarding the ultimate strategy for its use. On the

TABLE 1. SUMMARY TABLE FOR EXPERIMENTAL INVESTIGATIONS CITED WITHIN THE TEXT PERTAINING TO THE IMPACT OF SHEAR STRESS ON OSTEOGENIC AND ANGIOGENIC CELL DIFFERENTIATION

Shear stress (Pa)	Duration	Type of flow	Reactor type	Cell line	Culture surface/scaffold type	Prestress attachment period	Poststress culture period	Results	Reference
1	1 h	Oscillatory (1 Hz)	2D—parallel plate flow chamber	Nonhuman—C3H10T1/2 mesenchymal progenitor cells (murine)	Fibronectin-coated glass slides	48 h	30 min	Osteogenic	70
$1-2\times10^{-1}$	16 days	Steady	3D—perfusion bioreactor	Nonhuman—rat marrow stromal cells	Titanium fiber mesh scaffolds	7 days (adhered to scaffold 24 h before flow induction)	N/A	Osteogenic	43
$1-2$	3 min or 1 h (rest inserted periods of 10 s every 10 loading cycles)	Oscillatory (1 Hz)	2D—parallel plate flow chamber	Nonhuman—MC3T3-E1	Quartz or glass slides	48 h	N/A	Osteogenic	79
$5\times10^{-5}-5\times10^{-2}$	7 days	Steady	3D—perfusion bioreactor	Nonhuman—MC3T3-E1	Trabecular bone	24 h	N/A	Proliferation/Osteogenic	98
$5\times10^{-1}-2.5$	24 h (SS) or 7 days (pulsatile)	Steady (2.5 Pa) or Pulsatile (19 ± 12 Pa)	2D—parallel plate flow chamber or capillary cartridges	Human—HUVECs	Fibronectin coated coverslips or capillary cartridges	24 h	N/A	Angiogenic	115
1.2	8 days	Steady	2D—orbital shaker	Human—ASC	Gelatine-coated plates	24 h	N/A	Angiogenic	121
1.6	6 h	Steady	2D—cone and plate viscometer	Nonhuman—primary porcine aortic endothelial cells	Glass plates coated in laminin I	Confluency	N/A	Angiogenic	124
$1\times10^{-1}-5$	1, 4, 12, and 24 h	Steady	2D—cone and plate viscometer	Human—HUVECs and HCAECs	Gelatine-coated plates	24 h	N/A	Angiogenic	116
1.2	30 or 90 min	Steady	2D—parallel plate flow chamber	Human—BMSCs	Glass slides	24 h	N/A	Osteogenic	129
6.5×10^{-4}	6 days	Steady	3D—interstitial fluid flow chamber	Human—BECs and LECs	Fibrin gel matrices $\pm$ VEGF	18–24 h	N/A	Angiogenic	122
2.2×10^{-1}	48 h	Pulsatile (the systole of the roller pump was set to 0.3 s and the diastole to 0.5 s)	2D—compliant polyurethane microporous tube	Nonhuman—murine ES cells expressing the LacZ gene	Fibronectin coated	2 days	N/A	Angiogenic	130
2×10^{-2}	1 h every 8 h for a total of 24 h	Steady or pulsatile (2 Hz) or oscillatory (1 Hz)	3D—perfusion bioreactor	Nonhuman—MC3T3-E1	Collagen-GAG	6 days adherence before flow	N/A	Osteogenic	74

| 2	30 min	Steady	2D—parallel plate flow chamber	Human—osteoblasts	Glass slides	Until 80% confluency	0–24 h	Proliferation/ Osteogenic	95
6×10^{-1}	60 min	Pulsatile (5 Hz)	2D—parallel plate flow chamber	Nonhuman—goat AT-MSC	Polylysine-coated glass slides	24 h	N/A	Osteogenic	90
3.6–27×10^{-2}	30 min of shear every other day for 13 days	Steady	2D—radial flow device	Nonhuman—rBMSCs	Fibronectin-coated substrates	48 h	0 or 13 days	Osteogenic	93
1.6×10^{-1}	5, 30, or 120 min every 2 days, either 2 and 4 or 6, 8, 10, and 12	Steady	2D—parallel plate flow chamber	Nonhuman—rBMSC	Fibronectin-coated glass slides	24 h	2 or 8 days	Osteogenic	78
2.3×10^{-1}	24 h	Steady (intermitent 5 min on, 5 min off)	2D—parallel plate flow chamber	Nonhuman—rBMSC			13 days	Osteogenic	80
1 (140 pulses/ min, 26.4 mm Hg), 1.5 (250 pulses/min, 52.5 mm Hg) or 2.5 (390 pulses/min, 71.7 mm Hg)	24 h	Pulsatile	2D—cellco CELLMAX artificial capillary modules	Nonhuman—ovine fetoplacental artery endothelial cells	Fibronectin-coated permeable polyethylene capillaries	11–13 days	N/A	Angiogenic	123
1	2 h	Oscillatory (1 Hz)	2D—parallel plate flow chamber	Human—MSC	Quartz/0.01% poly-l-lysine-coated glass slides	3–5 days	24 h–3 days	Proliferation/ Osteogenic	94
6×10^{-1}	1 h	Pulsatile (5 Hz)	2D—parallel plate flow chamber	Human—primary human bone cells	Polylysine-coated glass slides	48 h	N/A	Osteogenic	96
3.9–6.4×10^{-1}	10 min	Pulsatile (0.39 Pa—3 Hz; 0.64 Pa—5 Hz)	2D—parallel plate flow chamber	Nonhuman—MC3T3-E1/ MLO-Y4 cells	Polylysine-coated glass slides	24 h	N/A	Osteogenic	71
1.5	24 h	Steady	2D—parallel plate flow chamber	Human—EECs, HUVECs and HMVECs	Gelatin-coated glass slides	48–72 h	24 h	Angiogenic	113
1.57×10^{-4}	21 days	Steady	3D—perfusion bioreactor	Nonhuman—murine K8 osteosarcoma	Collagen	24 h adherence before flow	N/A	Proliferation/ Osteogenic	97
1×10^{-2}–1.1	48 h or 7 days	Pulsatile (3 Hz)	2D—parallel plate flow chamber	Nonhuman—osteoprogenitor cells derived from rBMSCs	Tissue culture plates coated with cross-linked gelatin	14 days	N/A	Osteogenic	91
1×10^{-2}–5×10^{-1}	6 or 24 h	Steady	2D—rotating disk	Human—EPC	Fibronectin-coated culture dishes	5–6 days	N/A	Angiogenic	119

593

(continued)

TABLE 1. (CONTINUED)

Shear stress (Pa)	Duration	Type of flow	Reactor type	Cell line	Culture surface/scaffold type	Prestress attachment period	Poststress culture period	Results	Reference
2.8×10^{-1}	9 h	Steady	2D—parallel plate flow chamber	Nonhuman—MC3T3-E1	Glass slides	3 days	N/A	Osteogenic	131
2×10^{-2}	1 h every 8 h for a total of 1, 2, 4, 7, or 14 days—short rest periods of 10 s after every 10 s of flow during 1 h flow period	Steady	3D—perfusion bioreactor	Nonhuman—MC3T3-E1	Collagen-GAG	6 days adherence before flow	N/A	Osteogenic	75
2×10^{-2}	1 h every 8 h for 1, 2, 4, 7, or 14 days—short rest period of 5, 10, and 15 s after every 10 s of flow during 1 h flow period	Steady	3D—perfusion bioreactor	Nonhuman—MC3T3-E1	Collagen-GAG	6 days adherence before flow	N/A	Osteogenic	76
5×10^{-1}–2	1 min—2 h	Oscillatory (1 Hz)	2D—parallel plate flow chamber	Human—MSC	Quartz/glass slides	24 h	Up to 20 h	Proliferation/Osteogenic	83
2.3–4.3×10^{-1}	24 h	Steady or Pulsatile (0.015, 0.044, or 0.074 Hz)	2D—parallel plate flow chamber	Nonhuman—rBMSC	Fibronectin-coated glass slides	24 h	13 days	Osteogenic	77
1	1 h	Oscillatory (1 Hz)	2D—parallel plate flow chamber	Nonhuman—MC3T3-E1	Glass slides	48 h	30 min/1 h	Osteogenic	92
1–3×10^{-2}	4, 8, 16 days	Steady	3D—perfusion bioreactor	Nonhuman—rat MSC	Titanium fiber mesh scaffolds	7 days (adhered to scaffold 24 h before flow induction)	N/A	Osteogenic	85
5×10^{-3}	4, 8, 16 days	Steady	3D—perfusion bioreactor	Nonhuman—rat MSC	Poly(L-lactic acid) nonwoven scaffolds	7 days (adhered to scaffold 24 h before flow induction)	N/A	Proliferation/Osteogenic	86
1×10^{-2}–3	s/min	Steady	2D—parallel plate flow chamber	Nonhuman—MC3T3-E1	Glass slides	1–4 days	N/A	Osteogenic	132

Shear stress	Timing	Flow type	Reactor type	Cell source	Medium	Culture time	Additional timing	Application	Ref
5×10^{-1}	5 h	Pulsatile (1 Hz)	2D—parallel plate flow chamber	Nonhuman—MC3T3-E1	Glass slides	Until 80% confluency	N/A	Angiogenic	125
7×10^{-4} or 1.2	30 min per day for 1 or 2 days	Oscillatory (1 Hz)	3D—perfusion bioreactor	Nonhuman—MC3T3-E1	Calcium phosphate scaffold	Adhered to scaffold 24 h before flow induction	N/A	Osteogenic	81
1.5	6/12 h	Steady	2D—parallel plate flow chamber	Nonhuman—C3H10T1/2 mesenchymal progenitor cells (murine)	Collagen type I-coated tissue culture plates	Until 80% confluency	N/A	Angiogenic	126
1.5	6/24 h/48 h	Steady	2D—parallel plate flow chamber	Nonhuman—SMC line (P53LMA-CO1)	N/A	Until 80% confluency	5 h for tube formation assay	Angiogenic	127
1.2	24 h	Steady	2D—parallel plate flow chamber	Human—PDMCs	Glass slides	3 days	N/A	Angiogenic	117
1×10^{-2}–2.5×10^{-1}	Up to 21 days. Stress applied for 24 h every other day	Steady	2D—rotating disk	Human—EPC	Culture dishes coated with 100 g/mL of human fibronectin	3 days	N/A	Proliferation/Angiogenic	120
1.5×10^{-1}–1	24–72 h	Steady	2D—parallel plate flow chamber	Nonhuman—MGZ5 ES cells (murine)	Type IV collagen-coated dishes	48–72 h	<24 h	Proliferation/Angiogenic	133
5×10^{-1}	12 h	Steady	2D—parallel plate coculture flow chamber	Human—EPC (±hSMC)	10 mm-thick porous PET membrane	N/A	N/A	Angiogenic	118
2	3 min or 2 h	Oscillatory (1 Hz)	2D—parallel plate flow chamber	Nonhuman—MC3T3-E1	Glass/quartz slides	48 h	N/A	Osteogenic	82
1.2	24 h	Steady	2D—parallel plate flow chamber	Nonhuman—murine Sca1+ or ES cells	Collagen IV-coated plates	3–4 days	14 days for tube formation assay	Proliferation/Angiogenic	128
1×10^{-5}–1×10^{-4}	20 days	Steady	3D—perfusion bioreactor	Human—MSC	PET matrices	N/A	14 days for osteogenic differentiation	Proliferation/Osteogenic	87

Studies have been evaluated with respect to shear stress, flow type, reactor type, cell source, medium employed, and timing of shear stress application.

2D, two-dimensional; 3D, three-dimensional; ASC, adipose-derived stem cell; AT-MSC, adipose tissue-derived mesenchymal stem cell; BEC, blood endothelial cells; EEC, embryonic stem cell derived endothelial cell; EPC, endothelial progenitor cells; ES, embryonic stem cell; GAG, glycosaminoglycan; HCAEC, human coronary artery endothelial cells; HUVEC, human umbilical vein endothelial cells; LEC, lymphatic endothelial cells; N/A, not applicable; PDMC, placenta derived multipotent cells; PET, polyethylene terephthalate; rBMSCs, rat bone marrow stromal cells; SMC, smooth muscle cell; SS, steady state; VEGF, vascular endothelial growth factor.
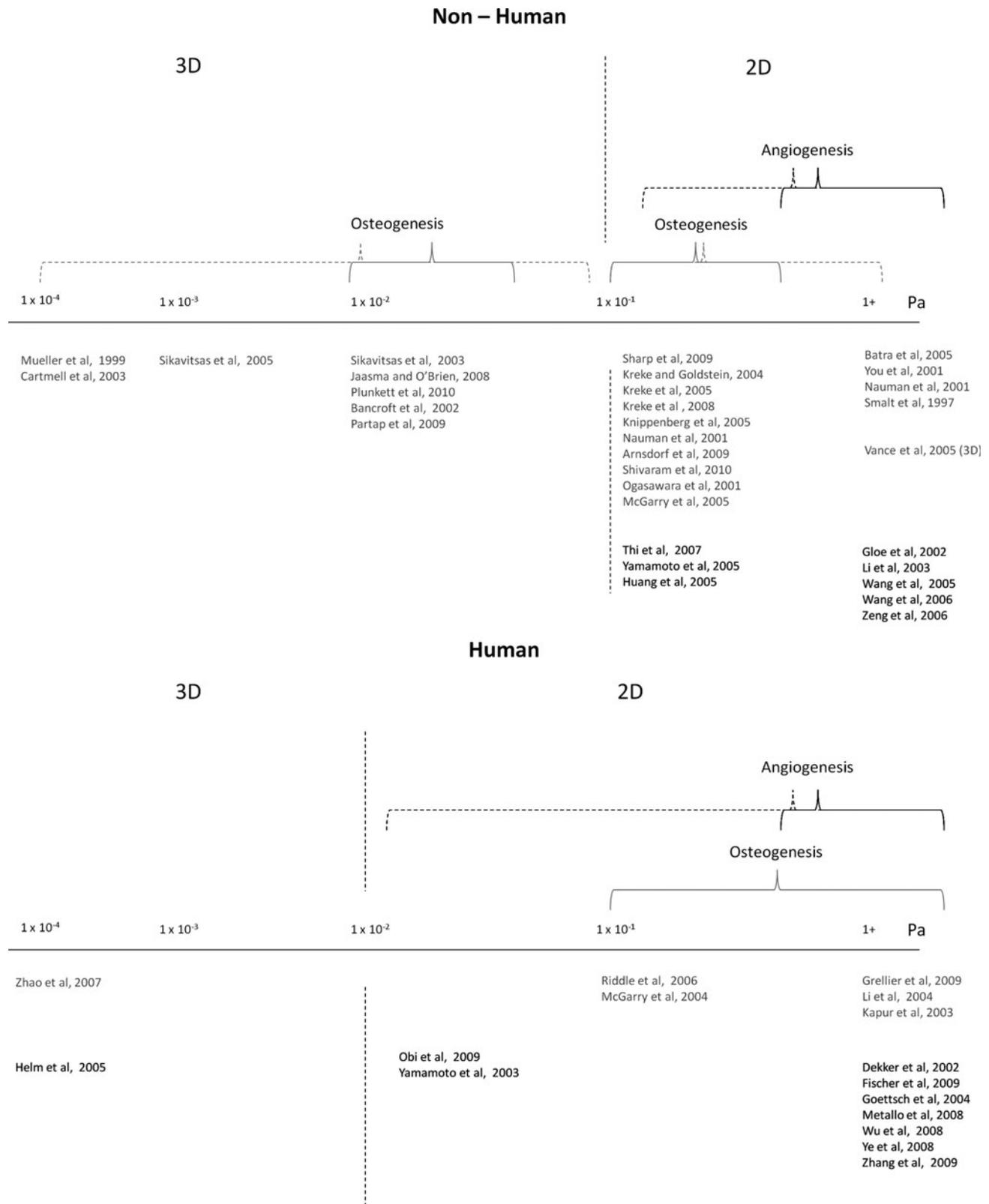
FIG. 3. Shear stress levels used in experiments for non-human and human cell lines for the induction of osteogenic and angiogenic lineages. Two-dimensional (2D) experiments relate to the application of shear stress on monolayer cultures using a variety of equipment setups: parallel plate flow chambers, radial flow or rotating disc devices, cone and plate viscometers, artificial capillaries, and microfluidic chambers. Three-dimensional (3D) experiments relate to experimental setups using highly porous scaffolds usually in the context of a perfusion bioreactor. References are located in accordance to the order of magnitude of shear stress applied in the investigation.

basis of the literature reviewed to date, creation of a tissue-engineered construct is likely to require two separate seeding phases and flow regimes. An initial phase will dynamically seed a progenitor cell line into the empty construct, providing a well distributed population reaching to the core of the scaffold. An initial static or low flow period for 48–72 h will follow encouraging cell attachment and proliferation. The primary flow regime will be angiogenic inducing in nature, a steady state flow of angiogenic media causing shear stress values an order of magnitude higher than those used for the osteogenic regime, for 3–5 days. Having established a nucleus of cells directed toward a vascular lineage, a second seeding phase, static in nature would be initiated with a new population of progenitor cells. These would be allowed to attach for a shorter period of time, 24 h (as the shear stresses caused by the second flow regime will be an order of magnitude or two lower than that used in the primary regime, and therefore the attachment strengths do not need to be so great). Application of a flow would be within the context of a rest-inserted regime, using osteo-inducing media, causing a shear stress distribution in the range 10^{-3}–10^{-2} Pa, thereby directing the progenitor cells toward an osteogenic fate. This second regime being applied for a shorter time frame of 24–48 h after which the graft would be implanted *in vivo*.

Conclusion

Directing the differentiation of progenitor cell lines through the use of a biomechanical cue such as shear stress is not a simple operation. The timing of its application, the flow type, the insertion of rest periods, and the magnitude of the stress itself can all influence the cellular response. It does appear that the use of nonhuman cell lines and 2D experimental apparatus can give indications regarding the trends in relation to some of these variables and provide insightful scientific understanding; however, direct translation to a clinically applicable 3D system for the generation of bone graft substitutes does not appear to be a straight forward undertaking. The future of shear stress-related investigations should clearly be targeted at filling the current void in knowledge surrounding 3D systems; identifying a strategy for creating cell seeded constructs committed toward a bone lineage with the potential for incorporating cells directed along an angiogenic lineage in an effort to further aid host integration.

Acknowledgments

Disclosure Statement

No competing financial interests exist.

References

1. Baksh, D., Davies, J.E., and Kim, S. Three-dimensional matrices of calcium polyphosphates support bone growth *in vitro* and *in vivo*. J Mater Sci Mater Med **9,** 743, 1998.
2. Jones, A.C., Arns, C.H., Sheppard, A.P., *et al.* Assessment of bone ingrowth into porous biomaterials using MICRO-CT. Biomaterials **28,** 2491, 2007.
3. Petite, H., Viateau, V., Bensaid, W., *et al.* Tissue-engineered bone regeneration. Nat Biotech **18,** 959, 2000.
4. Domaschke, H., Gelinsky, M., Burmeister, B., *et al. In vitro* ossification and remodeling of mineralized collagen I scaffolds. Tissue Eng **12,** 949, 2006.
5. Harley, B.A., Kim, H., Zaman, M.H., *et al.* Microarchitecture of three-dimensional scaffolds influences cell migration behavior via junction interactions. Biophys J **95,** 4013, 2008.
6. Corin, K.A., and Gibson, L.J. Cell contraction forces in scaffolds with varying pore size and cell density. Biomaterials **31,** 4835, 2010.
7. Burdett, E., Kasper, F.K., Mikos, A.G., and Ludwig, J.A. Engineering tumors: a tissue engineering perspective in cancer biology. Tissue Eng Part B Rev **16,** 351, 2010.
8. Moreau, J.E., Anderson, K., Mauney, J.R., *et al.* Tissue-engineered bone serves as a target for metastasis of human breast cancer in a mouse model. Cancer Res **67,** 10304, 2007.
9. Keogh, M., O' Brien, F., and Daly, J. A novel collagen scaffold supports human osteogenesis—applications for bone tissue engineering. Cell Tissue Res **340,** 169, 2010.
10. Farrell, E., Byrne, E., Fischer, J., *et al.* A comparison of the osteogenic potential of adult rat mesenchymal stem cells cultured in 2-D and on 3-D collagen glycosaminoglycan scaffolds. Technol Health Care **15,** 19, 2007.
11. Farrell, E., O'Brien, F.J., Doyle, P., *et al.* A collagen-glycosaminoglycan scaffold supports adult rat mesenchymal stem cell differentiation along osteogenic and chondrogenic routes. Tissue Eng **12,** 459, 2006.
12. Gugala, Z., and Gogolewski, S. The *in vitro* growth and activity of sheep osteoblasts on three-dimensional scaffolds from poly(L/DL-lactide) 80/20%. J Biomed Mater Res Part A **75A,** 702, 2005.
13. Ishaug-Riley, S.L., Crane-Kruger, G.M., Yaszemski, M.J., and Mikos, A.G. Three-dimensional culture of rat calvarial osteoblasts in porous biodegradable polymers. Biomaterials **19,** 1405, 1998.
14. Kim, H.J., Kim, U., Vunjak-Novakovic, G., Min, B., and Kaplan, D.L. Influence of macroporous protein scaffolds on bone tissue engineering from bone marrow stem cells. Biomaterials **26,** 4442, 2005.
15. St. Pierre, J., Gauthier, M., Lefebvre, L., and Tabrizian, M. Three-dimensional growth of differentiating MC3T3-E1 pre-osteoblasts on porous titanium scaffolds. Biomaterials **26,** 7319, 2005.
16. Tierney, C.M., Jaasma, M.J., and O'Brien, F.J. Osteoblast activity on collagen-GAG scaffolds is affected by collagen and GAG concentrations. J Biomed Mater Res Part A **91A,** 92, 2009.
17. Burr, D.B., Robling, A.G., and Turner, C.H. Effects of biomechanical stress on bones in animals. Bone **30,** 781, 2002.
18. Turner, C., Forwood, M., and Otter, M. Mechanotransduction in bone: do bone cells act as sensors of fluid flow? FASEB J **8,** 875, 1994.
19. Bikle, D.D., and Halloran, B.P. The response of bone to unloading. J Bone Miner Metab **17,** 233, 1999.
20. Morey, E., and Baylink, D. Inhibition of bone formation during space flight. Science **201,** 1138, 1978.
21. Zerwekh, J.E., Ruml, L.A., Gottschalk, F., and Pak, C.Y.C. The effects of twelve weeks of bed rest on bone histology, biochemical markers of bone turnover, and calcium homeostasis in eleven normal subjects. J Bone Miner Res **13,** 1594, 1998.
22. Burr, D.B., Milgrom, C., Fyhrie, D., *et al. In vivo* measurement of human tibial strains during vigorous activity. Bone **18,** 405, 1996.

23. Duncan, R.L., and Turner, C.H. Mechanotransduction and the functional response of bone to mechanical strain. Calcif Tissue Int **57,** 344, 1995.

24. Bouafsoun, A., Othmane, A., Kerkeni, A., Jaffrézic, N., and Ponsonnet, L. Evaluation of endothelial cell adherence onto collagen and fibronectin: a comparison between jet impingement and flow chamber techniques. Mater Sci Eng **C 26,** 260, 2006.

25. Kapur, R., and Rudolph, A.S. Cellular and cytoskeleton morphology and strength of adhesion of cells on self-assembled monolayers of organosilanes. Exp Cell Res **244,** 275, 1998.

26. Truskey, G.A., and Pirone, J.S. The effect of fluid shear stress upon cell adhesion to fibronectin-treated surfaces. J Biomed Mater Res **24,** 1333, 1990.

27. Truskey, G.A., and Proulx, T.L. Relationship between 3T3 cell spreading and the strength of adhesion on glass and silane surfaces. Biomaterials **14,** 243, 1993.

28. van Kooten, T., Schakenraad, J., van der Mei, H., and Busscher, H. Influence of substratum wettability on the strength of adhesion of human fibroblasts. Biomaterials **13,** 897, 1992.

29. van Kooten, T., Schakenraad, J., van der Mei, H., *et al.* Fluid shear induced endothelial cell detachment from glass—influence of adhesion time and shear stress. Med Eng Phys **16,** 506, 1994.

30. Wan, Y., Yang, J., Yang, J., Bei, J., and Wang, S. Cell adhesion on gaseous plasma modified poly-(-lactide) surface under shear stress field. Biomaterials **24,** 3757, 2003.

31. Wan, Y., Qu, X., Lu, J., *et al.* Characterization of surface property of poly(lactide-co-glycolide) after oxygen plasma treatment. Biomaterials **25,** 4777, 2004.

32. Xiao, Y., and Truskey, G. Effect of receptor-ligand affinity on the strength of endothelial cell adhesion. Biophys J **71,** 2869, 1996.

33. Deligianni, D.D., Katsala, N.D., Koutsoukos, P.G., and Missirlis, Y.F. Effect of surface roughness of hydroxyapatite on human bone marrow cell adhesion, proliferation, differentiation and detachment strength. Biomaterials **22,** 87, 2001.

34. Engler, A.J., Chan, M., Boettiger, D., and Schwarzbauer, J.E. A novel mode of cell detachment from fibrillar fibronectin matrix under shear. J Cell Sci **122,** 1647, 2009.

35. García, A.J., Ducheyne, P., and Boettiger, D. Quantification of cell adhesion using a spinning disc device and application to surface-reactive materials. Biomaterials **18,** 1091, 1997.

36. Garcia, A.J., Ducheyne, P., and Boettiger, D. Cell adhesion strength increases linearly with adsorbed fibronectin surface density. Tissue Eng **3,** 197, 1997.

37. Horbett, T.A., Waldburger, J.J., Ratner, B.D., and Hoffman, A.S. Cell adhesion to a series of hydrophilic-hydrophobic copolymers studies with a spinning disc apparatus. J Biomed Mater Res **22,** 383, 1988.

38. Goldstein, A.S., and DiMilla, P.A. Application of fluid mechanic and kinetic models to characterize mammalian cell detachment in a radial-flow chamber. Biotechnol Bioeng **55,** 616, 1997.

39. Goldstein, A.S., and DiMilla, P.A. Examination of membrane rupture as a mechanism for mammalian cell detachment from fibronectin-coated biomaterials. J Biomed Mater Res Part A **67A,** 658, 2003.

40. Furukawa, K.S., Ushida, T., Nagase, T., *et al.* Quantitative analysis of cell detachment by shear stress. Mater Sci Eng **C 17,** 55, 2001.

41. Christophis, C., Grunze, M., and Rosenhahn, A. Quantification of the adhesion strength of fibroblast cells on ethylene glycol terminated self-assembled monolayers by a microfluidic shear force assay. Phys Chem Chem Phys **12,** 4498, 2010.

42. Lu, H., Koo, L.Y., Wang, W.M., *et al.* Microfluidic shear devices for quantitative analysis of cell adhesion. Anal Chem **76,** 5257, 2004.

43. Bancroft, G.N., Sikavitsas, V.I., van den Dolder, J., *et al.* Fluid flow increases mineralized matrix deposition in 3D perfusion culture of marrow stromal osteoblasts in a dose-dependent manner. Proc Natl Acad Sci U S A **99,** 12600, 2002.

44. Goldstein, A.S., Juarez, T.M., Helmke, C.D., Gustin, M.C., and Mikos, A.G. Effect of convection on osteoblastic cell growth and function in biodegradable polymer foam scaffolds. Biomaterials **22,** 1279, 2001.

45. Ishaug, S.L., Crane, G.M., Miller, M.J., *et al.* Bone formation by three-dimensional stromal osteoblast culture in biodegradable polymer scaffolds. J Biomed Mater Res **36,** 17, 1997.

46. Martin, I., Obradovic, B., Freed, L.E., and Vunjak-Novakovic, G. Method for quantitative analysis of glycosaminoglycan distribution in cultured natural and engineered cartilage. Ann Biomed Eng **27,** 656, 1999.

47. Martin, I., Wendt, D., and Heberer, M. The role of bioreactors in tissue engineering. Trends Biotechnol **22,** 80, 2004.

48. Bonvin, C., Overney, J., Shieh, A.C., Dixon, J.B., and Swartz, M.A. A multichamber fluidic device for 3D cultures under interstitial flow with live imaging: development, characterization, and applications. Biotechnol Bioeng **105,** 982, 2010.

49. Jaasma, M.J., Plunkett, N.A., and O'Brien, F.J. Design and validation of a dynamic flow perfusion bioreactor for use with compliant tissue engineering scaffolds. J Biotechnol **133,** 490, 2008.

50. Zhao, F., and Ma, T. Perfusion bioreactor system for human mesenchymal stem cell tissue engineering: dynamic cell seeding and construct development. Biotechnol Bioeng **91,** 482, 2005.

51. Wendt, D., Jakob, M., and Martin, I. Bioreactor-based engineering of osteochondral grafts: from model systems to tissue manufacturing. J Biosci Bioeng **100,** 489, 2005.

52. Porter, B.D., Lin, A.S., Peister, A., Hutmacher, D., and Guldberg, R.E. Noninvasive image analysis of 3D construct mineralization in a perfusion bioreactor. Biomaterials **28,** 2525, 2007.

53. Yannas, I.V., Lee, E., Orgill, D.P., Skrabut, E.M., and Murphy, G.F. Synthesis and characterization of a model extracellular matrix that induces partial regeneration of adult mammalian skin. Proc Natl Acad Sci U S A **86,** 933, 1989.

54. Al-Munajjed, A.A., and O'Brien, F.J. Influence of a novel calcium-phosphate coating on the mechanical properties of highly porous collagen scaffolds for bone repair. J Mech Behav Biomed Mater **2,** 138, 2009.

55. Al-Munajjed, A.A., Plunkett, N.A., Gleeson, J.P., *et al.* Development of a biomimetic collagen-hydroxyapatite scaffold for bone tissue engineering using a SBF immersion technique. J Biomed Mater Res Part B Appl Biomater **90B,** 584, 2009.

56. Cunniffe, G., Dickson, G., Partap, S., Stanton, K., and O'Brien, F. Development and characterisation of a collagen

nano-hydroxyapatite composite scaffold for bone tissue engineering. J Mater Sci Mater Med **21,** 2293, 2010.

57. O'Brien, F.J., Harley, B.A., Yannas, I.V., and Gibson, L. Influence of freezing rate on pore structure in freeze-dried collagen-GAG scaffolds. Biomaterials **25,** 1077, 2004.

58. Mandal, B.B., and Kundu, S.C. Non-bioengineered silk fibroin protein 3D scaffolds for potential biotechnological and tissue engineering applications. Macromol Biosci **8,** 807, 2008.

59. Boschetti, F., Raimondi, M.T., Migliavacca, F., and Dubini, G. Prediction of the micro-fluid dynamic environment imposed to three-dimensional engineered cell systems in bioreactors. J Biomech **39,** 418, 2006.

60. Jungreuthmayer, C., Donahue, S.W., Jaasma, M.J., *et al.* A comparative study of shear stresses in collagen-glycosaminoglycan and calcium phosphate scaffolds in bone tissue-engineering bioreactors. Tissue Eng Part A **15,** 1141, 2009.

61. Porter, B., Zauel, R., Stockman, H., Guldberg, R., and Fyhrie, D. 3-D computational modeling of media flow through scaffolds in a perfusion bioreactor. J Biomech **38,** 543, 2005.

62. Hutmacher, D.W., Sittinger, M., and Risbud, M.V. Scaffold-based tissue engineering: rationale for computer-aided design and solid free-form fabrication systems. Trends Biotechnol **22,** 354, 2004.

63. Hollister, S.J. Porous scaffold design for tissue engineering. Nat Mater **4,** 518, 2005.

64. Sachlos, E., and Czernuszka, J.T. Making tissue engineering scaffolds work. Review: the application of solid freeform fabrication technology to the production of tissue engineering scaffolds. Eur Cell Mater **5,** 29, 2003.

65. Peltola, S.M., Melchels, F.P.W., Grijpma, D.W., and Kellomäki, M. A review of rapid prototyping techniques for tissue engineering purposes. Ann Med **40,** 268, 2008.

66. Jacobs, C.R., Temiyasathit, S., and Castillo, A.B. Osteocyte mechanobiology and pericellular mechanics. Annu Rev Biomed Eng **12,** 369, 2010.

67. Hoffman, B.D., and Crocker, J.C. Cell mechanics: dissecting the physical responses of cells to force. Annu Rev Biomed Eng **11,** 259, 2009.

68. Janmey, P.A., and McCulloch, C.A. Cell mechanics: integrating cell responses to mechanical stimuli. Annu Rev Biomed Eng **9,** 1, 2007.

69. Heino, J. The collagen receptor integrins have distinct ligand recognition and signaling functions. Matrix Biol **19,** 319, 2000.

70. Arnsdorf, E.J., Tummala, P., Kwon, R.Y., and Jacobs, C.R. Mechanically induced osteogenic differentiation—the role of RhoA, ROCKII and cytoskeletal dynamics. J Cell Sci **122,** 546, 2009.

71. McGarry, J.G., Klein-Nulend, J., and Prendergast, P.J. The effect of cytoskeletal disruption on pulsatile fluid flow-induced nitric oxide and prostaglandin E2 release in osteocytes and osteoblasts. Biochem Biophys Res Commun **330,** 341, 2005.

72. Annaz, B., Hing, K., Kayser, M., Buckland, T., and Silvio, L.D. Porosity variation in hydroxyapatite and osteoblast morphology: a scanning electron microscopy study. J Microsc **215,** 100, 2004.

73. McMahon, L. The effect of cylic tensile loading and growth factors on the chondrogenic differentiation of bone-marrow derived mesenchymal stem cells in a collagen-glycosaminoglycan scaffold. Thesis submitted to Trinity College Dublin, Dublin, Ireland, 2007.

74. Jaasma, M.J., and O'Brien, F.J. Mechanical stimulation of osteoblasts using steady and dynamic fluid flow. Tissue Eng Part A **14,** 1213, 2008.

75. Partap, S., Plunkett, N., Kelly, D., and O'Brien, F. Stimulation of osteoblasts using rest periods during bioreactor culture on collagen-glycosaminoglycan scaffolds. J Mater Sci Mater Med **21,** 2325, 2010.

76. Plunkett, N.A., Partap, S., and O'Brien, F.J. Osteoblast response to rest periods during bioreactor culture of collagen-glycosaminoglycan scaffolds. Tissue Eng Part A **16,** 943, 2010.

77. Sharp, L., Lee, Y., and Goldstein, A. Effect of low-frequency pulsatile flow on expression of osteoblastic genes by bone marrow stromal cells. Ann Biomed Eng **37,** 445, 2009.

78. Kreke, M.R., Huckle, W.R., and Goldstein, A.S. Fluid flow stimulates expression of osteopontin and bone sialoprotein by bone marrow stromal cells in a temporally dependent manner. Bone **36,** 1047, 2005.

79. Batra, N.N., Li, Y.J., Yellowley, C.E., *et al.* Effects of short-term recovery periods on fluid-induced signaling in osteoblastic cells. J Biomech **38,** 1909, 2005.

80. Kreke, M.R., Sharp, L.A., Lee, Y.W., and Goldstein, A.S. Effect of intermittent shear stress on mechanotransductive signaling and osteoblastic differentiation of bone marrow stromal cells. Tissue Eng Part A **14,** 529, 2008.

81. Vance, J., Galley, S., Liu, D.F., and Donahue, S.W. Mechanical stimulation of MC3T3 osteoblastic cells in a bone tissue-engineering bioreactor enhances prostaglandin E2 release. Tissue Eng **11,** 1832, 2005.

82. You, J., Reilly, G.C., Zhen, X., *et al.* Osteopontin gene regulation by oscillatory fluid flow via intracellular calcium mobilization and activation of mitogen-activated protein kinase in MC3T3-E1 osteoblasts. J Biol Chem **276,** 13365, 2001.

83. Riddle, R.C., Taylor, A.F., Genetos, D.C., and Donahue, H.J. MAP kinase and calcium signaling mediate fluid flow-induced human mesenchymal stem cell proliferation. Am J Physiol Cell Physiol **290,** C776, 2006.

84. You, J., Yellowley, C.E., Donahue, H.J., *et al.* Substrate deformation levels associated with routine physical activity are less stimulatory to bone cells relative to loading-induced oscillatory fluid flow. J Biomech Eng **122,** 387, 2000.

85. Sikavitsas, V.I., Bancroft, G.N., Holtorf, H.L., Jansen, J.A., and Mikos, A.G. Mineralized matrix deposition by marrow stromal osteoblasts in 3D perfusion culture increases with increasing fluid shear forces. Proc Natl Acad Sci U S A **100,** 14683, 2003.

86. Sikavitsas, V., Bancroft, G., Lemoine, J., *et al.* Flow perfusion enhances the calcified matrix deposition of marrow stromal cells in biodegradable nonwoven fiber mesh scaffolds. Ann Biomed Eng **33,** 63, 2005.

87. Zhao, F., Chella, R., and Ma, T. Effects of shear stress on 3-D human mesenchymal stem cell construct development in a perfusion bioreactor system: experiments and hydrodynamic modeling. Biotechnol Bioeng **96,** 584, 2007.

88. Alvarez-Barreto, J.F., and Sikavitsas, V.I. Improved mesenchymal stem cell seeding on RGD-modified poly(L-lactic acid) scaffolds using flow perfusion. Macromol Biosci **7,** 579, 2007.

89. Alvarez-Barreto, J., Linehan, S., Shambaugh, R., and Sikavitsas, V. Flow perfusion improves seeding of tissue engineering scaffolds with different architectures. Ann Biomed Eng **35,** 429, 2007.

90. Knippenberg, M., Helder, M.N., Doulabi, B.Z., *et al.* Adipose tissue-derived mesenchymal stem cells acquire bone cell-like responsiveness to fluid shear stress on osteogenic stimulation. Tissue Eng **11,** 1780, 2005.

91. Nauman, E.A., Satcher, R.L., Keaveny, T.M., Halloran, B.P., and Bikle, D.D. Osteoblasts respond to pulsatile fluid flow with short-term increases in PGE2 but no change in mineralization. J Appl Physiol **90,** 1849, 2001.

92. Shivaram, G.M., Kim, C.H., Batra, N.N., *et al.* Novel early response genes in osteoblasts exposed to dynamic fluid flow. Philos Trans R Soc A Math Phys Eng Sci **368,** 605, 2010.

93. Kreke, M.R., and Goldstein, A.S. Hydrodynamic shear stimulates osteocalcin expression but not proliferation of bone marrow stromal cells. Tissue Eng **10,** 780, 2004.

94. Li, Y.J., Batra, N.N., You, L., *et al.* Oscillatory fluid flow affects human marrow stromal cell proliferation and differentiation. J Orthop Res **22,** 1283, 2004.

95. Kapur, S., Baylink, D.J., and William Lau, K.H. Fluid flow shear stress stimulates human osteoblast proliferation and differentiation through multiple interacting and competing signal transduction pathways. Bone **32,** 241, 2003.

96. McGarry, J.G., Klein-Nulend, J., Mullender, M.G., and Prendergast, P.J. A comparison of strain and fluid shear stress in stimulating bone cell responses—a computational and experimental study. FASEB J **19,** 482, 2004.

97. Mueller, S.M., Mizuno, S., Gerstenfeld, L.C., and Glowacki, J. Medium perfusion enhances osteogenesis by murine osteosarcoma cells in three-dimensional collagen sponges. J Bone Miner Res **14,** 2118, 1999.

98. Cartmell, S., Porter, B.D., García, A.J., and Guldberg, R.E. Effects of medium perfusion rate on cell-seeded three-dimensional bone constructs *in vitro*. Tissue Eng **9,** 1197, 2003.

99. Holtorf, H.L., Datta, N., Jansen, J.A., and Mikos, A.G. Scaffold mesh size affects the osteoblastic differentiation of seeded marrow stromal cells cultured in a flow perfusion bioreactor. J Biomed Mater Res Part A **74A,** 171, 2005.

100. Holtorf, H.L., Jansen, J.A., and Mikos, A.G. Flow perfusion culture induces the osteoblastic differentiation of marrow stromal cell-scaffold constructs in the absence of dexamethasone. J Biomed Mater Res Part A **72A,** 326, 2005.

101. Holtorf, H.L., Sheffield, T.L., Ambrose, C.G., Jansen, J.A., and Mikos, A.G. Flow perfusion culture of marrow stromal cells seeded on porous biphasic calcium phosphate ceramics. Ann Biomed Eng **33,** 1238, 2005.

102. Jungreuthmayer, C., Jaasma, M., Al-Munajjed, A., *et al.* Deformation simulation of cells seeded on a collagen-GAG scaffold in a flow perfusion bioreactor using a sequential 3D CFD-elastostatics model. Med Eng Phys **31,** 420, 2009.

103. Jaasma, M.J., Jackson, W.M., Tang, R.Y., and Keaveny, T.M. Adaptation of cellular mechanical behavior to mechanical loading for osteoblastic cells. J Biomech **40,** 1938, 2007.

104. Jackson, W.M., Jaasma, M.J., Tang, R.S., and Keaveny, T.M. Mechanical loading by fluid shear is sufficient to alter the cytoskeletal composition of osteoblastic cells. Am J Physiol Cell Physiol **295,** C1005, 2008.

105. Niklason, L.E., Gao, J., Abbott, W.M., *et al.* Functional arteries grown *in vitro*. Science **284,** 489, 1999.

106. Niklason, L.E., Abbott, W., Gao, J., *et al.* Morphologic and mechanical characteristics of engineered bovine arteries. J Vasc Surg **33,** 628, 2001.

107. Syedain, Z.H., Weinberg, J.S., and Tranquillo, R.T. Cyclic distension of fibrin-based tissue constructs: evidence of adaptation during growth of engineered connective tissue. Proc Natl Acad Sci **105,** 6537, 2008.

108. Huang, C.C., Hagar, K.L., Frost, L.E., Sun, Y., and Cheung, H.S. Effects of cyclic compressive loading on chondrogenesis of rabbit bone-marrow derived mesenchymal stem cells. Stem Cells **22,** 313, 2004.

109. Lima, E., Bian, L., Ng, K., *et al.* The beneficial effect of delayed compressive loading on tissue-engineered cartilage constructs cultured with TGF-[beta]3. Osteoarthritis Cartilage **15,** 1025, 2007.

110. Mauck, R.L., Soltz, M.A., Wang, C.C.B., *et al.* Functional tissue engineering of articular cartilage through dynamic loading of chondrocyte-seeded agarose gels. J Biomech Eng **122,** 252, 2000.

111. Mauck, R., Byers, B., Yuan, X., and Tuan, R. Regulation of cartilaginous ECM gene transcription by chondrocytes and MSCs in 3D culture in response to dynamic loading. Biomech Model Mechanobiol **6,** 113, 2007.

112. Benhardt, H.A., and Cosgriff-Hernandez, E.M. The role of mechanical loading in ligament tissue engineering. Tissue Eng Part B Rev **15,** 467, 2009.

113. Metallo, C.M., Vodyanik, M.A., Pablo, J.J.D., Slukvin, I.I., and Palecek, S.P. The response of human embryonic stem cell-derived endothelial cells to shear stress. Biotechnol Bioeng **100,** 830, 2008.

114. Zhang, P., Baxter, J., Vinod, K., Tulenko, T.N., and Di Muzio, P.J. Endothelial differentiation of amniotic fluid-derived stem cells: synergism of biochemical and shear force stimuli. Stem Cells Dev **18,** 1299, 2009.

115. Dekker, R.J., van Soest, S., Fontijn, R.D., *et al.* Prolonged fluid shear stress induces a distinct set of endothelial cell genes, most specifically lung Kruppel-like factor (KLF2). Blood **100,** 1689, 2002.

116. Goettsch, W., Augustin, H.G., and Morawietz, H. Down-regulation of endothelial ephrinB2 expression by laminar shear stress. Endothelium **11,** 259, 2004.

117. Wu, C., Chao, Y., Chen, C., *et al.* Synergism of biochemical and mechanical stimuli in the differentiation of human placenta-derived multipotent cells into endothelial cells. J Biomech **41,** 813, 2008.

118. Ye, C., Bai, L., Yan, Z., Wang, Y., and Jiang, Z. Shear stress and vascular smooth muscle cells promote endothelial differentiation of endothelial progenitor cells via activation of Akt. Clin Biomech **23,** S118, 2008.

119. Obi, S., Yamamoto, K., Shimizu, N., *et al.* Fluid shear stress induces arterial differentiation of endothelial progenitor cells. J Appl Physiol **106,** 203, 2009.

120. Yamamoto, K., Takahashi, T., Asahara, T., *et al.* Proliferation, differentiation, and tube formation by endothelial progenitor cells in response to shear stress. J Appl Physiol **95,** 2081, 2003.

121. Fischer, L.J., McIlhenny, S., Tulenko, T., *et al.* Endothelial differentiation of adipose-derived stem cells: effects of endothelial cell growth supplement and shear force. J Surg Res **152,** 157, 2009.

122. Helm, C.E., Fleury, M.E., Zisch, A.H., Boschetti, F., and Swartz, M.A. Synergy between interstitial flow and VEGF directs capillary morphogenesis *in vitro* through a gradient amplification mechanism. Proc Natl Acad Sci U S A **102,** 15779, 2005.

123. Li, Y., Zheng, J., Bird, I.M., and Magness, R.R. Effects of pulsatile shear stress on nitric oxide production and endothelial cell nitric oxide synthase expression by ovine fetoplacental artery endothelial cells. Biol Reprod **69,** 1053, 2003.

124. Gloe, T., Sohn, H.Y., Meininger, G.A., and Pohl, U. Shear stress-induced release of basic fibroblast growth factor

from endothelial cells is mediated by matrix interaction via integrin αVβ3. J Biol Chem **277,** 23453, 2002.

125. Thi, M.M., Iacobas, D.A., Iacobas, S., and Spray, D.C. Fluid shear stress upregulates vascular endothelial growth factor gene expression in osteoblasts. Ann N Y Acad Sci **1117,** 73, 2007.

126. Wang, H., Riha, G.M., Yan, S., *et al.* Shear stress induces endothelial differentiation from a murine embryonic mesenchymal progenitor cell line. Arterioscler Thromb Vasc Biol **25,** 1817, 2005.

127. Wang, H., Yan, S., Chai, H., *et al.* Shear stress induces endothelial transdifferentiation from mouse smooth muscle cells. Biochem Biophys Res Commun **346,** 860, 2006.

128. Zeng, L., Xiao, Q., Margariti, A., *et al.* HDAC3 is crucial in shear- and VEGF-induced stem cell differentiation toward endothelial cells. J Cell Biol **174,** 1059, 2006.

129. Grellier, M., Bareille, R., Bourget, C., and Amédéé, J. Responsiveness of human bone marrow stromal cells to shear stress. J Tissue Eng Regen Med **3,** 302, 2009.

130. Huang, H., Nakayama, Y., Qin, K., *et al.* Differentiation from embryonic stem cells to vascular wall cells under *in vitro* pulsatile flow loading. J Artif Organs **8,** 110, 2005.

131. Ogasawara, A., Arakawa, T., Kaneda, T., *et al.* Fluid shear stress induced cyclooxygenase-2 expression is mediated by C/EBPβ, cAMP-response element binding protein, and AP-1 in osteoblastic MC3T3-E1 cells. J Biol Chem **276,** 7048, 2001.

132. Smalt, R., Mitchell, F.T., Howard, R.L., and Chambers, T.J. Induction of No and prostaglandin E2 in osteoblasts by wall shear stress but not mechanical strain. Am J Physiol Endocrinol Metab **273,** E751, 1997.

133. Yamamoto, K., Sokabe, T., Watabe, T., *et al.* Fluid shear stress induces differentiation of FLK-1-positive embryonic stem cells into vascular endothelial cells *in vitro.* Am J Physiol Heart Circ Physiol **288,** H1915, 2005.

Address correspondence to:
Fergal J. O'Brien, Ph.D.
Department of Anatomy
Royal College of Surgeons in Ireland
123 St. Stephen's Green
Dublin 2
Ireland

E-mail: fjobrien@rcsi.ie